5050–5060 *Nucleic Acids Research, 2008, Vol. 36, No. 15* *Published online 28 July 2008*
doi:10.1093/nar/gkn459

Assembling of G-strands into novel tetra-molecular parallel G4-DNA nanostructures using avidin–biotin recognition

Natalia Borovok[1], Natalie Iram[1], Dragoslav Zikich[1], Jamal Ghabboun[2], Gideon I. Livshits[2], Danny Porath[2,3] and Alexander B. Kotlyar[1,4,*]

[1]Department of Biochemistry, George S. Wise Faculty of Life Sciences, Tel Aviv University, Ramat Aviv, 69978, [2]Physical Chemistry Department, [3]Center for Nanoscience and Nanotechnology, The Hebrew University, Jerusalem 91904, Israel and [4]The Center for Nanoscience and Nanotechnology, Tel Aviv University

Received May 4, 2008; Revised July 1, 2008; Accepted July 2, 2008

ABSTRACT

We describe a method for the preparation of novel long (hundreds of nanometers), uniform, inter-molecular G4-DNA molecules composed of four parallel G-strands. The only long continuous G4-DNA reported so far are intra-molecular structures made of a single G-strand. To enable a tetra-molecular assembly of the G-strands we developed a novel approach based on avidin–biotin biological recognition. The steps of the G4-DNA production include: (i) Enzymatic synthesis of long poly(dG)-poly(dC) molecules with biotinylated poly(dG)-strand; (ii) Formation of a complex between avidin-tetramer and four biotinylated poly(dG)-poly(dC) molecules; (iii) Separation of the poly(dC) strands from the poly(dG)-strands, which are connected to the avidin; (iv) Assembly of the four G-strands attached to the avidin into tetra-molecular G4-DNA. The average contour length of the formed structures, as measured by AFM, is equal to that of the initial poly(dG)-poly(dC) molecules, suggesting a tetra-molecular mechanism of the G-strands assembly. The height of tetra-molecular G4-nanostructures is larger than that of mono-molecular G4-DNA molecules having similar contour length. The CD spectra of the tetra- and mono-molecular G4-DNA are markedly different, suggesting different structural organization of these two types of molecules. The tetra-molecular G4-DNA nanostructures showed clear electrical polarizability. This suggests that they may be useful for molecular electronics.

INTRODUCTION

G-rich DNA sequences containing runs of guanines (dG) can form G-quadruplex structures. These structures, commonly named G4-DNA, are comprised of stacked tetrads; each of the tetrads arises from the planar association of four guanines by Hoogsteen hydrogen bonding. The potential biological role of G4-DNA stimulated investigation of the physico-chemical properties of these structures. Most of the studies have been performed using short (16–32 bases) G-rich telomeric oligonucleotides that are stable only in the presence of stabilizing cations (K^+ or Na^+) (1–5); removal of the cations results in a complete unfolding of the G-quadruplexes. Short G-rich oligonucleotides were shown to assemble spontaneously into long molecular wires in the presence of proper monovalent cations (6–8). These wires comprise a large number of G-oligonucleotide fragments assembled in a tetra-helix fashion and not covalently connected to one another. G-quadruplex structures are very polymorphic and are characterized by various molecularity, topology and strand orientation (9). G-quadruplex DNA may be formed from one, two and four separate DNA strands, thus termed mono-, bi- and tetra-molecular G4-DNA, correspondingly (10–15).

In the tetra-molecular structures, each one of the four strands contributes one G-residue to form a tetrad. In the bi-molecular structures, each strand contributes two guanines to each tetrad and in the mono-molecular structures all the G-residues are coming from the same strand. G4-DNA forming sequences were found at the ends of chromosomes in the so-called telomeric regions, as well as in transcriptional regulatory regions in several oncogenes (16,17), immunoglobulin heavy chain switch

*To whom correspondence should be addressed. Tel: 972 3 6407138; Fax: 972 3 6406834; Email: s2shak@post.tau.ac.il
Correspondence may also be addressed to Danny Porath. Tel: 972 2 6586948; Fax: 972 2 6586987; Email: porath@chem.ch.huji.ac.il

regions, some promoter regions, minisatellites and ribosomal DNA. Besides their physiological relevance, guanine tetrads have drawn attention in the nanotechnology field, since they were proposed as building blocks of molecular nanowires for nanoelectronics (18). G4-wires comprise a large number (hundreds) of stacked guanine tetrads, thus providing better conditions for π overlap compared to the base-pairs of the canonical double-stranded DNA and higher structural rigidity and stability under various conditions (e.g. boiling, DNase). A high guanine content, having the lowest ionization potential among the DNA bases, increases the probability of charge migration through G4-wires (19–21). These properties make G4-wires attractive candidates for nanoelectronics applications. So far, the structures made of short G-oligonucleotide sequences resulted in non-uniform polymers having gaps (non-covalently bonded backbone) between oligonucleotide fragments along the formed wires (6,8,22). These drawbacks limit the mechanical stability and stacking in so-produced wires and strongly reduce their ability to conduct current, therefore limiting their application in nanoelectronics.

We have recently reported the synthesis of novel continuous mono-molecular G quadruplex DNA nanostructures composed of single self-folded poly(G) strands containing hundreds of stacked tetrads (18). These nanostructures are characterized by a narrow length distribution and contain no gaps in their backbone. We have also demonstrated that these mono-molecular wires are characterized by higher charge polarizability, as compared to double-stranded DNA (23). Mono-molecular quadruplexes, made of single intra-molecular folded G-strands, are the only long continuous G4-DNA nanostructures reported so far. Long G-quadruplexes composed of four long parallel G-strands might possess improved electric properties with respect to mono-molecular G-wires and better ability to insert interruptions in specific positions along the molecule. However, uniform inter-molecular G4-wires do not form spontaneously in solution. At high concentration, which is required for the tetra-molecular assembly, G-strands aggregate into bundles comprised of a large number of strands. In order to avoid the formation of aggregates and enable only the tetra-molecular G-strand folding, we developed an approach based on the avidin–biotin interaction. The basic idea behind this approach is that the avidin-tetramer brings together four G-strands, end-labeled with biotin, therefore enabling their tetra-molecular folding at low molecular concentrations.

Avidin is a glycoprotein, which consists of four identical subunits, each capable of tight biotin binding (24–28). The interaction between avidin and biotin is the strongest non-covalent interaction known in biology. The complex between the protein and the ligand is stable under various experimental conditions: pH from 2 to 13, high temperatures and presence of organic solvents (29–32). These unique characteristics of the complex, together with commercial availability of biotinylated nucleic acids and proteins, make the biotin–avidin system a universal tool for assembling proteins and nucleic acids (25,28,33,34).

Here we present a novel avidin–biotin-based method that enables the formation of long, parallel, tetra-molecular G4-DNA structures. The morphology of the structures was measured by AFM and their properties were characterized by HPLC, electrophoresis, CD and absorption spectroscopy. We showed that the CD spectrum and the morphology of the tetra-molecular structures differ from those of the mono-molecular G4-DNA.

We demonstrated, by electrostatic force microscopy (EFM), that tetra-molecular G4-DNA nanostructures show polarizability, as their intra-molecular counterpart.

MATERIALS AND METHODS

Materials

Unless otherwise stated, the reagents were obtained from Sigma–Aldrich (USA) and were used without further purification. The 2′-deoxyribonucleoside 5′-triphosphate (dGTP) was purchased from Sigma–Aldrich (USA). Klenow fragment exonuclease minus of DNA polymerase I from *E.coli* lacking the 3′→5′ exonuclease activity (Klenow exo$^-$) was purchased from Fermentas (Lithuania).

DNA samples

The oligonucleotides were purchased from Alpha DNA (Montreal, Canada). In biotinylated $(dG)_{12}$-oligonucleotide (5′biotin–$(dG)_{12}$) the biotin residue is linked to the terminal base at the 5′-end. All the oligonucleotides were purified by HPLC using Agilent 1100 HPLC system with a photodiode array detector. The $(dC)_{12}$-oligonucleotides were purified on an ion-exchange Western Analytical Products (USA) PolyWax LP column (4.6 × 200 mm, 5 μm, 300 Å). The oligonucleotides were eluted from the column in 10% Acetonitrile with linear K-Pi (pH 7.5) gradient from 20 mM to 0.5 M for 1 h with flow rate of 0.8 ml/min. The $(dG)_{12}$- and 5'biotin–$(dG)_{12}$-oligonucleotides were purified using an ion-exchange HiTrap QHP column (5 × 1 ml) from Amersham-Biosciences (Sweden) at pH 13. Elution was conducted in 0.1 M NaOH and 10% acetonitrile with a linear NaCl gradient from 0.5 to 1 M for 1 h at a flow rate of 0.7 ml/min. Peaks were identified by their retention times obtained from the absorbance at 260 nm. Purified oligonucleotides were desalted using pre-packed Sephadex G-25 DNA-Grade columns (Amersham-Biosciences). In order to create template-primer for enzymatic synthesis the purified 5′biotin–$(dG)_{12}$-oligonucleotides were incubated with their complementary counterparts in 0.1 M NaOH at a molar ratio of 1 : 1 for 15 min and further dialyzed against 20 mM Tris-Acetate buffer, pH 7.5, for 2 h. All the oligonucleotides were quantified spectrophotometrically using their respective extinction coefficients. The concentrations of the $(dG)_{12}$ and $(dC)_{12}$ were calculated using extinction coefficients of 11.7 and 7.5 $mM^{-1}\,cm^{-1}$ at 260 nm, respectively (35).

DNA polymerase assays

The standard reaction contained 60 mM KPi, pH 7.4, 5 mM $MgCl_2$, 5 mM DTT and 1.5 mM of dGTP and 1.5 mM dCTP, 0.2 μM Klenow exo$^-$ and 0.2 μM template-primer, 5′biotin–$(dG)_{12}$-$(dC)_{12}$. The reaction was triggered by the addition of the enzyme. The incubation was performed at 37°C for time intervals indicated in the figure legends. The reaction was terminated by the addition of EDTA to a final concentration of 20 mM. Reaction products were analyzed by size exclusion HPLC and by an agarose gel electrophoresis.

HPLC separation of the polymerase products

5′biotin–poly(dG)-poly(dC) produced during the enzymatic synthesis (see above) were separated from nucleotides and other reaction components of the synthesis using size-exclusion HPLC. The separation was achieved with a TSK-gel G-DNA PW HPLC column (7.8 × 300 mm) from TosoHaas (Japan) by isocratic elution with 20 mM Tris–Acetate at pH 8.5 for 30 min at a flow rate of 0.5 ml/min. Injection volumes were 20–170 μl. The separation was conducted with an Agilent 1100 HPLC system with a photodiode array detector. Peaks were identified by their retention times obtained from the absorbance at 260 nm.

Preparation of avidin–Poly(dG)-Poly(dC) complex

Egg-white avidin (0.2 μM) was incubated with 5′biotin–poly(dG)-poly(dC) (1 μM in molecules) in 0.2 M CAPS buffer (pH 10.5) and 0.5 M NaCl, for 4 h at 25°C. The concentration of avidin was calculated using extinction coefficient of 97.4 $mM^{-1}cm^{-1}$ at 280 nm (36). The avidin–5′biotin–poly(dG)-poly(dC) complex was purified from unbound 5′biotin–poly(dG)-poly(dC) molecules using size-exclusion HPLC. The separation was achieved with a TSK-gel G-DNA PW HPLC column (7.8 × 300 mm) from TosoHaas (Japan) by isocratic elution with 20 mM Tris–Acetate (pH 8.5), 0.5 M NaCl, for 30 min at a flow rate of 0.5 ml/min. Peaks were identified by their retention times obtained from the absorbance at 260 nm. The purity of the avidin–5′biotin–poly(dG)-poly(dC) complex was confirmed by agarose gel electrophoresis.

Preparation of avidin–G4-DNA complex

The avidin–5′biotin–poly(dG)-poly(dC) complex obtained as described above was pretreated for 20 min at room temperature in 0.1 M LiOH in order to dissociate poly(dG)-strands connected to avidin from poly(dC)-strands. The separation was carried out with a size-exclusion TSK-gel G-DNA PW HPLC column (7.8 × 300 mm) from TosoHaas (Japan) by isocratic elution with 0.1 M LiOH for 30 min at a flow rate of 0.5 ml/min. Peaks were identified by their retention times obtained from the absorbance at 260 nm. The avidin–poly(dG) fraction was collected and dialyzed against 20 mM LiCl for 4 h. During the dialysis the pH of the solution was reduced and the G-strands folded. The dialyzed complex was chromatographed on TSK-gel G-DNA PW HPLC column (7.8 × 300 mm) from TosoHaas (Japan) in 0.1 M Tris–Acetate (pH 7.5). The main fraction was collected; the late fraction enriched with tri-molecular avidin–5′biotin–poly(dG) complex was discarded.

CD and absorption spectroscopy

CD spectra were recorded at 25°C with an Aviv Model 202 series (Aviv Instrument Inc., USA) Circular Dichroism Spectrometer. Each spectrum was recorded from 220 to 340 nm and was an average of 5 scans. Absorption spectra of the synthesized products were recorded with a Jasco V-630 spectrophotometer (Japan).

AFM imaging

Atomic force microscopy was performed on the molecules adsorbed onto mica surfaces. A 20 μl of 1.0–2.0 nM (in molecules) Avidin–DNA and G4-DNA samples in 50 mM HEPES or Tris–Acetate, pH 7.5, containing 0.5–2.0 mM $MgCl_2$ were incubated on a freshly cleaved moskovite mica plates for 5 min, washed with distilled water and dried with nitrogen gas. AFM images were obtained with two systems: (i) a Solver PRO (NT-MDT, Russia) AFM in a non-contact (tapping) mode using 130 μm long Si-gold-coated cantilevers (NT-MDT, Russia) with resonance frequency of 119–180 kHz. (ii) Images and electrostatic polarizability were measured with Nanotec Electronica S.L. Madrid, in dynamic mode. Soft cantilevers (OMCL-RC800PSA, Olympus Optical Co., Ltd) of nominal force constant 0.3 Nm^{-1}, resonance frequency 75–80 kHz and tip radius 15–20 nm were used (the tip radius was measured with a scanning electron microscope). The cantilever was oscillated at its resonance frequency while the amplitude and the phase, relative to the oscillatory driving force, were measured through the tip deflection signal as detected by the photo-detector. The feedback was performed on the amplitude signal channel. The images were 'flattened' (each line of the image was fitted to a 2nd-order polynomial, and the polynomial was then subtracted from the image line) by the AFM's image processing software. The images were analyzed and visualized using a Nanotec Electronica S.L (Madrid) WSxM imaging software (37).

Electrostatic force microscopy (EFM) polarizability measurements

The electrostatic polarizability of the molecules was checked by EFM using various methods described in details in (23,38). The EFM results presented here were measured in retrace mode with a tip lift of 30 nm above the topography set point height (and above the effective VDW force range, where the electrical interaction is dominant) at 0, −4 and +4 V applied to the tip. The phase shift signal that is compared for the different molecules at the various voltages is integrated from the cross-sections along the molecule. For electrical functionality all the cantilevers used in this work were sputter-coated with AuPd at a nominal thickness of 15–30 nm. As a result the resonance frequency was reduced to ~60 kHz. While scanning, the cantilevers were oscillated at low amplitude of up to

20 nm peak-to-peak, resulting in a low stored energy that increased the measurement sensitivity.

Gel electrophoresis

The products of the polymerase synthesis were analyzed by 0.7% agarose gel electrophoresis at room temperature at 130 V for 1 h. TAE buffer was used for the agarose preparation and as a running buffer. The dimensions of the agarose gel were 10×10 cm with 2×4 mm 14-wells. The gel was stained with ethidium bromide (0.5 μg/ml) and visualized with a Bio Imaging System (302 nm).

RESULTS

Preparation and characterization of the avidin–Poly(dG)-Poly(dC) complexes

We have synthesized double-stranded poly(dG)-poly(dC) molecules composed of C-homopolymers and 5′-end biotin-labeled G-homopolymers, as described in 'Materials and methods' section. The polymerase synthesis, conducted essentially as described in (39) yielded 1.4 kb 5′biotin–poly(dG)-poly(dC) molecules characterized by a narrow length distribution (Figure 1, lane 2). Incubation of the synthesized 5′biotin–poly(dG)-poly(dC) molecules with the avidin-tetramer as described in 'Materials and methods' section, results in the formation of the complex between the DNA and the protein. Figure 1 shows gel electrophoretic patterns of complexes obtained during incubation of 5′biotin–poly(dG)-poly(dC) with avidin at different DNA to avidin ratios. As can be seen in the Figure 1, incubation of the avidin-tetramer with twice the amount of 5′biotin–poly(dG)-poly(dC) yields a complex with a mass of ~3 kb (Figure 1, lane 3) and thus corresponds to two 5′biotin–poly(dG)-poly(dC) molecules joined together by avidin. The increase of the ratio between the DNA to the protein leads to the formation of higher molecular mass (~5 and ~6 kb) complexes corresponding to three and four 5′biotin–poly(dG)-poly(dC) molecules linked together (Figure 1, lanes 4–6), respectively. Increasing the ratio above four results in a mixture of the saturated avidin–DNA complex, comprising of four 5′biotin–poly(dG)-poly(dC) molecules (tetra-molecular complex), and single 5′biotin–poly(dG)-poly(dC) molecules not grouped by avidin (Figure 1, lane 6). A minor quantity of the tri-molecular complex is present together with the tetra-molecular one even in the mixture containing a large (5 and more) excess of DNA over the protein (Figure 1, lane 6). The tetra-molecular complex prepared at a 5:1 ratio between 5′biotin–poly(dG)-poly(dC) and avidin (Figure 1) was purified from the excess of unbound DNA using size-exclusion HPLC. The elution profile (Figure 2A) shows two major peaks. The first one, eluted between 12 and 14 min, corresponds to the avidin–4[biotin–poly(dG)-poly(dC)] complex; and the second peak, eluted between 14 and 16 min, to 5′biotin–poly(dG)-poly(dC) not linked to avidin. The molecular composition and the purity of molecules eluted in the first peak were analyzed by agarose gel-electrophoresis (Figure 2B). The electrophoretic analysis clearly shows that the complex is completely separated

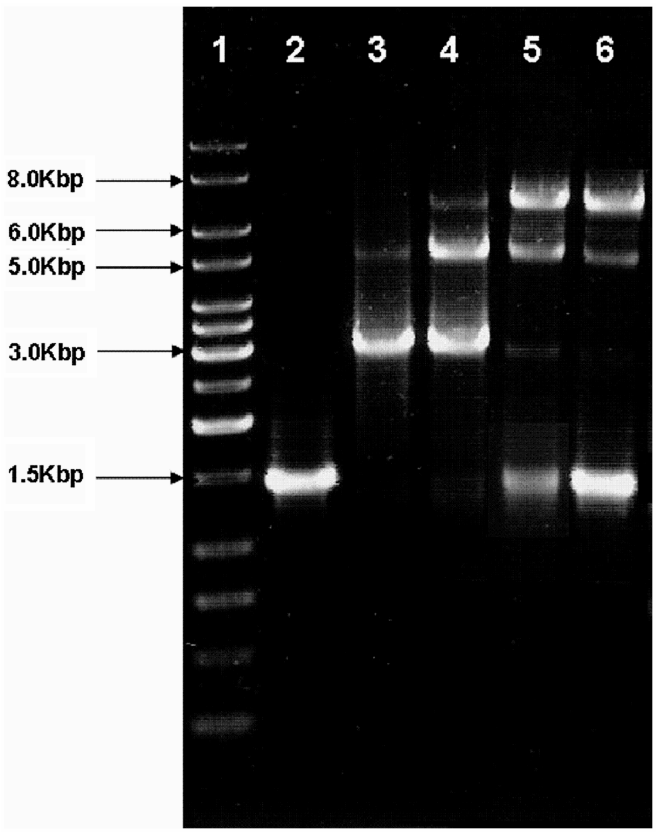

Figure 1. Mobility of poly(dG)-poly(dC)–avidin complexes in 0.7% Agarose gel. A 1.4 kb 5′biotin–poly(dG)-poly(dC) (lane 2) was incubated with avidin at molar ratios of 2, 3, 4 and 5, as described in 'Materials and methods' section—lanes 3, 4, 5 and 6, correspondingly. Lane 1 is 1 kb DNA Ladder.

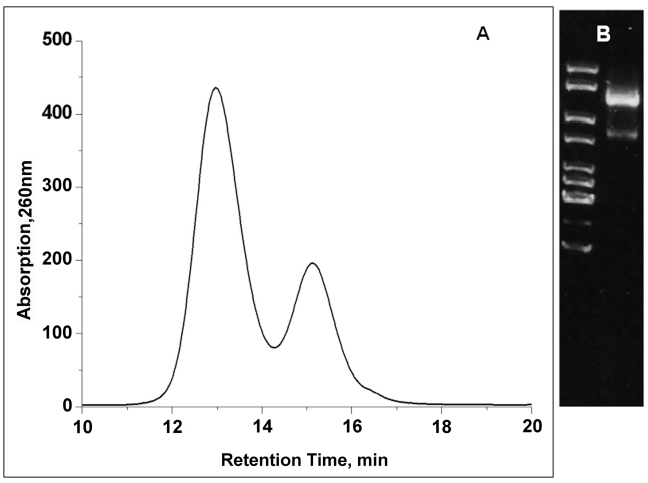

Figure 2. HPLC purification of avidin–5′biotin–poly(dG)-poly(dC) complex. (**A**) Size-exclusion HPLC separation of avidin–5′biotin–poly(dG)-poly(dC) complex from unbound 5′biotin–poly(dG)-poly(dC). The separation was carried out on the G-DNA PW column in 20 mM Tris–Acetate buffer, pH 7.4 and 0.5 M NaCl, as described in 'Materials and methods' section. (**B**) 0.7% agarose gel electrophoresis of the purified avidin–5′biotin–poly(dG)-poly(dC). The complex was eluted from the column between 12 and 14 min.

from the unbound 5′-biotin–poly(dG)-poly(dC) molecules; the quality of the separation obtained with the HPLC technique is, however, not sufficient to purify the tetra-molecular complex from the tri-molecular one. The latter complex is seen as a minor band (Figure 2B) below the major band, corresponding to the tetra-molecular complex, on the electrophoresis gel image.

The 4[biotin–poly(dG)-poly(dC)]–avidin complex is stable at high ionic strength and does not undergo any changes for weeks at 4°C. Reducing the ionic strength, however, results in its fast disintegration (Figure 3). The incubation of the saturated complex, which correspond to 3 kb bands (Figure 3, lane 3), in 20 mM Tris–HCl for 2 h results in almost complete disappearance of the bands and the appearance of a new band corresponding to 0.7 kb band (Figure 3, lane 4). These results suggest that the complex dissociates into poly(dG)-poly(dC) molecules not grouped by avidin. The dissociation can be reversed by addition of NaCl; in the presence of 0.5 M (or higher) concentration of the salts the complexes reassemble and appear as 2 and 3 kb bands on the gel (Figure 3, lane 5).

The HPLC-purified tetra-molecular 1.4 kb 4[biotin–poly(dG)-poly(dC)]–avidin complexes were visualized by AFM. The complexes, collected from the HPLC column (Figure 2A), were deposited on a freshly cleaved mica surface and measured by AFM, as described in 'Materials and methods' section. Figure 4 presents an AFM image of the complex. The avidin is seen in the image as a bright sphere to which four linear poly(dG)-poly(dC) molecules are attached (Figure 4A). As can be seen in Figure 4A, there are a few molecules containing three arms, corresponding to an avidin–3[poly(dG)-poly(dC)] complex. The presence of a minor quantity (~20%) of this complex is consistent with our gel-electrophoresis results (Figure 2B). The contour length distributions of poly(dG)-poly(dC) molecules attached to avidin is presented in Figure 4B. The average contour lengths of more than 450 analyzed DNA molecules is 323 ± 54 nm. We have recently demonstrated (40) that poly(dG)-poly(dC) molecules are immobilized on mica in a form related to the A-form DNA duplex, in contrast to poly(dA)-poly(dT) and random sequence DNA which are immobilized in a form corresponding to the B-form DNA duplex. The estimated contour length of the poly(dG)-poly(dC) is rather close to that expected for a double-stranded A-form DNA composed of 1400 bp (364 nm) assuming a rise per base pair of 2.6 Å (40).

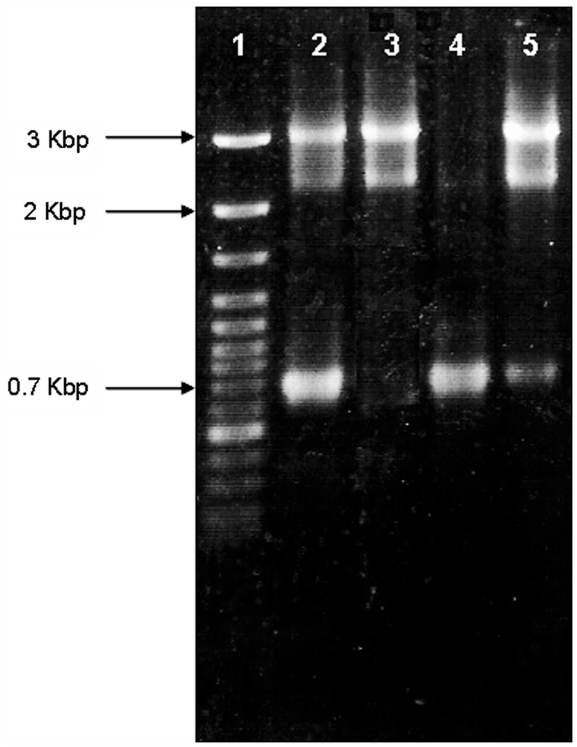

Figure 3. Dissociation and re-association of 0.7 kb poly(dG)-poly(dC)–avidin complex. The 5′biotin–poly(dG)-poly(dC)–avidin complex was prepared at a poly(dG)-poly(dC) to avidin (tetramer) ratio of 5, as described in 'Materials and methods' section (lane 2) and was further purified by HPLC as shown in Figure 2 (lane 3). The complex was passed through a Sephadex G-25 column equilibrated with 2 mM Tris–HCl (pH 7.4) and was further incubated in the column buffer for 2 h at 25°C (lane 4). A 0.5 M NaCl (final concentration) was added and the incubation was continued for 24 h (lane 5). Lane 1 is 100 bp DNA Ladder.

Preparation and characterization of the avidin-G4 complex

A complex between four 1.4 kb biotin–poly(dG)-poly(dC) molecules and avidin, prepared as described in 'Material and methods' section (and the caption of Figure 2), was used as the starting material for tetra-molecular G4-DNA nanostructures production. The poly(dC) strands were separated from the biotin–poly(dG) strands connected to avidin during the size-exclusion HPLC of 4[biotin–poly(dG)-poly(dC)]–avidin at high pH. At pH > 12.5 the poly(dG) and the poly(dC) strands composing poly(dG)-poly(dC) molecules are separated from one another. The size-exclusion chromatography of the complex in 0.1 M LiOH results in a separate elution of G-strands connected to the avidin and C-strands (Figure 5). The good separation quality achieved by the size-exclusion HPLC is due to the difference in molecular masses of the 4[poly(dG)]–avidin complex containing four G-strands compared to single C-strand. The first peak eluted from the column between 12.5 and 14.5 min corresponds to G-strands grouped together by avidin, while the second peak eluted between 15.5 and 18 min corresponds to C-strands. The absorption spectra of fractions eluted with the first and the second peaks fit nicely with those of G- and C-nucleotides, respectively. The poly(dG) fraction collected from the HPLC column was dialyzed against 20 mM LiCl for 4 h. During the dialysis the pH of the solution was reduced from 13.0 to 8.0 and the strands underwent folding into G4-DNA structures. The dialyzed molecules were passed through a size-exclusion HPLC column, as described in 'Materials and methods' section. The G4-avidin complex was collected from the HPLC column and was imaged by AFM. As seen in the AFM image (Figure 6A), each molecule is composed of a linear segment corresponding to the DNA and a brighter sphere corresponding to the avidin. The average contour length of more than 400 single analyzed molecules is equal to

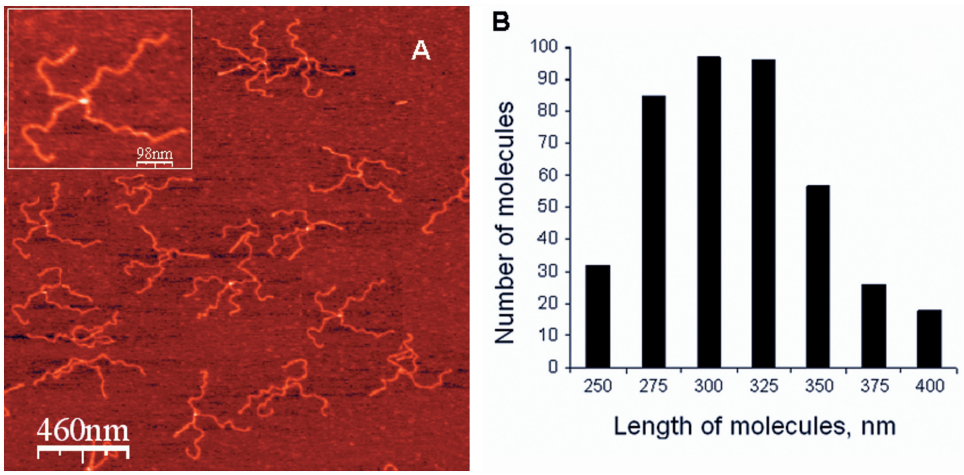

Figure 4. AFM image of avidin–5′biotin–poly(dG)-poly(dC). (**A**) AFM image of 1.4 kb 5′biotin–poly(dG)-poly(dC)–avidin complex. The complex was formed at a biotin–poly(dG)-poly(dC) to avidin ratio of 5, as described in 'Materials and methods' section, and was further purified by HPLC as shown in Figure 2. Molecules were deposited on mica and measured, as described in 'Materials and methods' section. The avidin is seen as a brighter spot in the middle of the complex. (**B**) Statistical contour length analysis of more than 400-well separated DNA molecules attached to avidin. Inset: Enlargement of a 5′biotin–poly(dG)-poly(dC)–avidin complex.

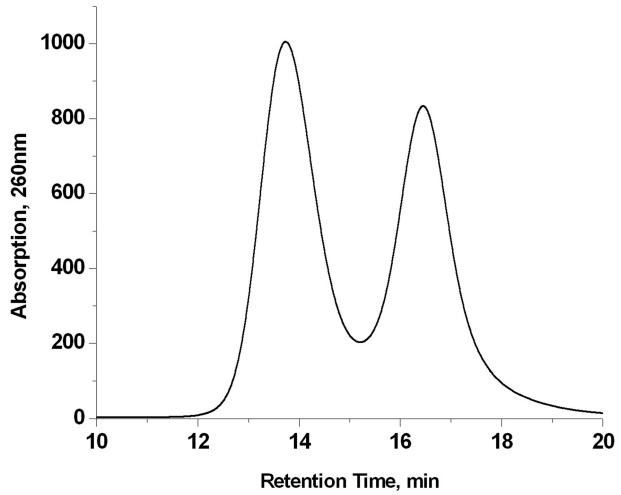

Figure 5. Size-exclusion HPLC separation of four-molecular 1.4 kb 5′-biotin–poly(dG)–avidin complex from poly(dC) in base. The 5′biotin–poly(dG)-poly(dC)–avidin complex was prepared at a poly(dG)-poly(dC) to avidin ratio of 5, as described in 'Materials and methods' section, and was further purified by HPLC as shown in Figure 2. The complex was pretreated for 20 min at room temperature in 0.1 M LiOH in order to dissociate poly(dC)-strands from poly(dG)-strands connected to avidin. The separation was achieved with a size-exclusion G-DNA-PW HPLC column (7.8 × 300 mm) by isocratic elution with 0.1 M LiOH for 30 min at a flow rate of 0.5 ml/min.

275 ± 25 nm (Figure 6C). Statistical AFM morphology imaging analysis shows that the contour length of the G4-DNA molecules is somewhat shorter, although within the experimental error, to the length of the initial poly(dG)-poly(dC) (323 ± 54 nm, see Figure 4) suggesting a tetra-molecular mechanism of the G-strands assembling.

The morphology of the tetra-molecular G-quadruplexes reported here was compared with the morphology of mono-molecular G4-DNA reported by us earlier (18). The latter mono-molecular quadruplexes are prepared by folding a single G-strand four times as described in (18). For the sake of comparison, mono-molecular G-quadruplexes were made from the same amount of G-bases (~5.5 kb) as the tetra-molecular ones (4 × 1.4 kb). Note that in mono-molecular G-quadruplexes all G-bases belong to the same chain, while in tetra-molecular G-quadruplexes they are equally distributed between the four chains composing the DNA. Moreover, in the 4-folded molecules every two strands run in opposite directions, while in the latter molecules all the four strands run in the same 3′–5′ direction. Both types of molecules were deposited on a freshly cleaved mica surface and measured by AFM. Figure 6A and B shows images and C and D comparative contour length analyses of the tetra- and mono-molecular G4-quadruplexes, correspondingly. The statistical analysis (Figure 6C and D) shows that the contour length of the tetra-molecular quadruplexes (275 ± 25 nm) is shorter than that of the mono-molecular ones (351 ± 44 nm). The average height of the tetra-molecular quadruplexes (2.2 ± 0.2 nm) is noticeably larger than that of the mono-molecular quadruplexes (1.0 ± 0.2 nm). The apparent heights were extracted from cross-sections of hundreds of molecules of each type measured under identical conditions. Figure 7 presents height profiles taken along the marked lines of two typical tetra-molecular single G4-wires. The height of the avidin is approximately equal to 5 nm, while the height of the G4-DNA connected to it is approximately equal to 2.5 nm. It is clearly evident from Figure 7 that the height of the DNA in the complex is not influenced by the protein; the same height was measured close (2.5 nm) to and opposite to the site of the avidin's attachment.

CD spectra of tetra- and mono-molecular G-quadruplexes are shown in Figure 8. As seen in the figure, the CD spectrum of the mono-molecular quadruplexes is characterized by a positive band at 256 nm and a negative band at 276 nm, while the spectrum of tetra-molecular quadruplexes has only a positive band at

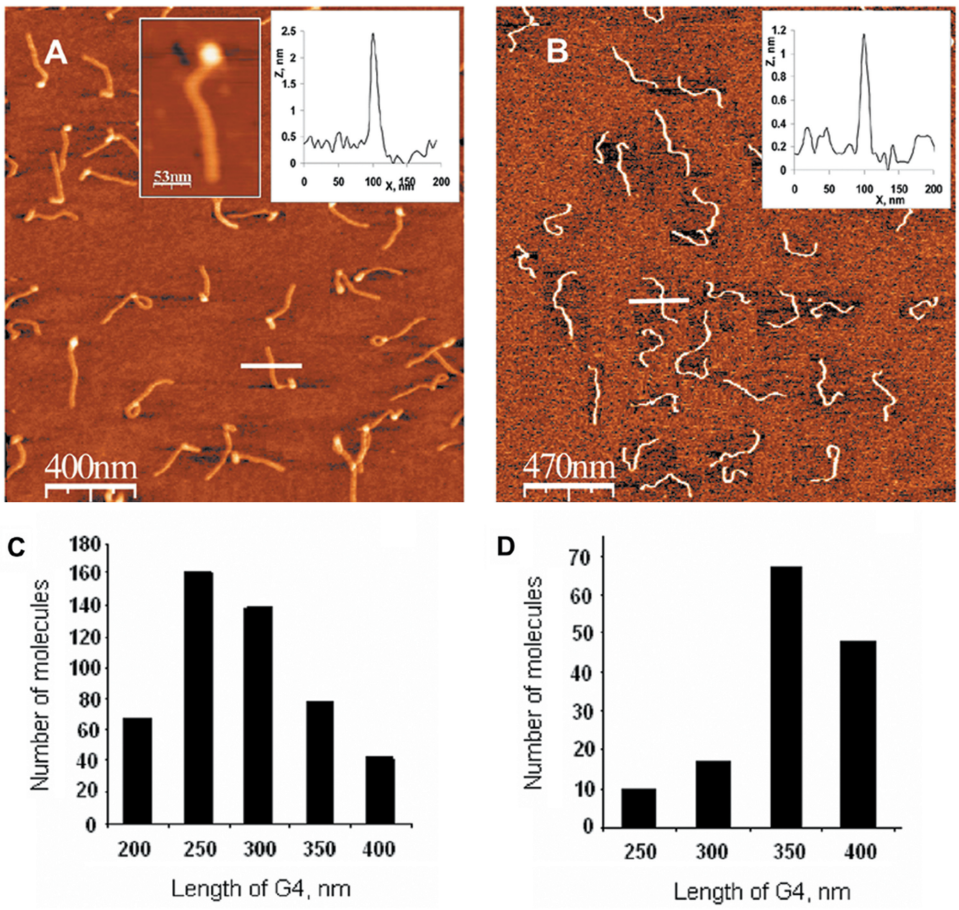

Figure 6. Comparison between the tetra- and mono-molecular G-quadruplexes. AFM images of tetra-molecular (Inset: enlargement of a tetra-molecular complex) (**A**) and monomolecular (**B**) G-quadruplexes. Tetra-molecular G-quadruplexes were prepared, as described in 'Materials and methods' section, using complex of four 1.4 kb 5′biotin–poly(dG)-poly(dC) molecules connected to avidin as starting material. Monomolecular G-quadruplexes were prepared as described in 'Introduction' section using 5.5 kb G-strand. Both types of molecules were deposited on mica under the same conditions. Statistical contour length analysis of tetra-molecular (**C**) and monomolecular (**D**) G-quadruplexes. More than 300 single-well separated molecules of each type were subjected to the statistic analysis. Inset: Enlargement of one of the tetra-molecular G4-DNA molecules.

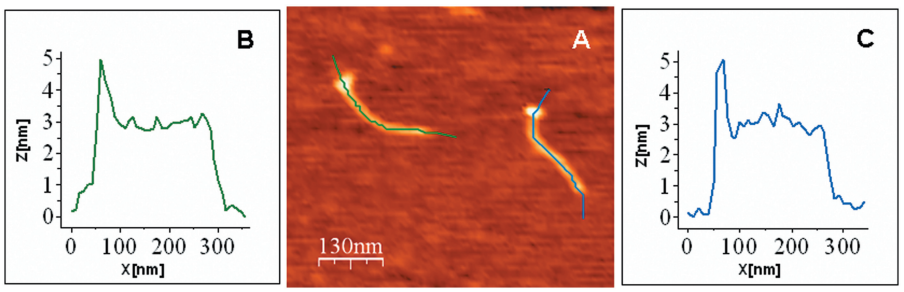

Figure 7. The height profiles of tetra-molecular G-quadruplexes. AFM images of tetra-molecular G4-wires (**A**) and their height profiles (**B** and **C**). Tetra-molecular G-quadruplexes were prepared, as described in 'Materials and methods' section, using complex of four 1.4 kb 5′biotin–poly(dG)-poly(dC) molecules connected to avidin as starting material.

260 nm (Figure 8, lines 1 and 2, respectively). The base-induced unfolding of the tetra-molecular structures results in the complete disappearance of the original positive CD band at 260 nm (Figure 8, line 4). We have shown earlier (18) that long mono-molecular structures are stable without K^+ or Na^+ in contrast to short tetraplexes, which formation takes place only in the presence of these cations. Here we show that the same is true for tetra-molecular quadruplexes; these structures are very stable in the absence of K^+(Na^+) and do not undergo any noticeable changes during weeks. Addition of K^+ to tetra-molecular G-quadruplexes prepared in the absence

of K^+ results in a slight (6 nm) shift of the maximum at 260 nm and in appearance of a weak negative band at 278 nm in the CD spectrum (Figure 8, compare curves 1 and 3).

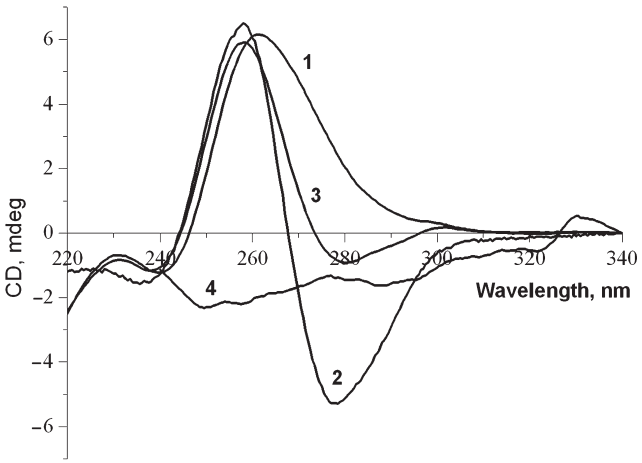

Figure 8. CD spectrometry of the G4-DNA. CD spectra of 200 nM tetra-molecular G-quadruplexes in 50 mM Tris-Acetate, pH 7.5 (line 1) in the presence of 10 mM KCl (line 3), and in the presence of 0.1 M LiOH (line 4). CD spectra of 200 nM monomolecular G-quadruplexes (line 2). Tetra-molecular G-quadruplexes were prepared, as described in 'Materials and methods' section. Monomolecular G-quadruplexes were prepared as described in 'Introduction' section using 5.5 kb G-strand.

Electrostatic force microscopy characterization of the avidine-G4 complex

An efficient non-contact and non-invasive way to identify polarizable objects, usually conducting materials with AFM, is electrostatic force microscopy (EFM) (23,38). In this method the phase shift between the induced and actual tip oscillations is recorded, thus providing a sensitive indication for the tip and sample electrostatic interaction, e.g. due to charge mobility or polarizability. When performing an EFM measurement, a voltage is applied to a metallized tip after raising it above the Van der Waals (VDW) interaction height (~10 nm) while the feedback is disabled. Attractive forces between the conductive tip and the probed object in both positive and negative bias voltages indicate a polarization response of the charge carriers in the measured object to the electric field. In our measurement scheme, attractive forces are reflected as dark areas in the phase image.

In Figure 9 we demonstrate that the biotin–avidine-G4 complex shows clear polarizability. Figure 9A shows topography of two molecules. Cross-sections taken on one of the molecules (continuous line, Figure 9B) and on the avidin (dotted line, Figure 9C) show heights of 2.2 and 4.5 nm respectively. The phase shift image of the same scan area as in Figure 9A during scanning 30 nm above the imaging set-point (with the same oscillation amplitude) is shown in Figure 9D, F and H for +4, 0 and −4 V, respectively, with corresponding average cross-sections in E, G and I. The dark appearance of the

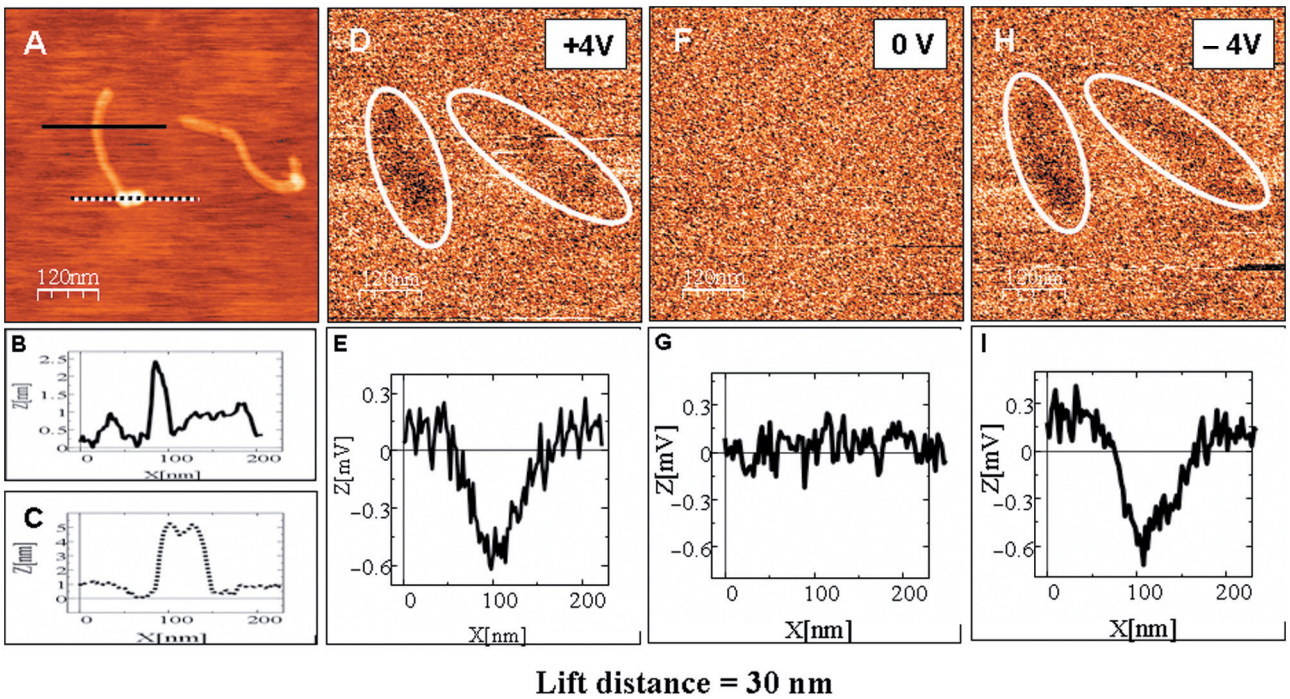

Figure 9. EFM measurements of avidin–biotin–G4-DNA. (**A**) A topography image of two complexes, where the avidin is the larger and brighter end of the molecules. (**B** and **C**) Cross-sections on the DNA and on avidin fragments of the complex from A (the molecule on the left) correspondingly. (**D**, **F** and **H**) Phase shift images taken 30 nm above the imaging set-point (with the same oscillation amplitude) with +4, 0 and −4 V, respectively, applied to the tip. The dark appearance of molecules in D and H indicates attraction between the molecules and the biased tip for both positive and negative voltages and therefore polarizability. At 0 V there is no detected interaction between the molecules and the tip. (**E**, **G** and **I**) Present an average on all the cross-sections along the left molecule from A measured at +4, 0 and −4 V correspondingly. The attractive interaction is clearly observed for ±4 V and no interaction is seen at 0 V.

molecules in the phase shift images, when ±4 V are applied, as expected, no molecules are seen at zero-bias. This suggests that the molecules are good candidates for conductivity measurements and if the wires will be found conductive, they will be very useful for nanoelectronic applications, as nanoelectronic wires.

DISCUSSION

We described here the procedure for preparation of novel long continuous tetra-molecular G4-wires based on avidin–biotin interaction. An avidin-tetramer, that can bind up to four biotin molecules (24–28), was used to bring together four G-strands, end-labeled with biotin and enabled their tetra-molecular folding. The avidin–biotin complex is extremely stable under various experimental conditions (pH from 2 to 13, high temperatures, presence of organic solvents) (29–32) and is particularly useful for preparation of tetra-molecular G4-wires. The procedure of the G4-wires production consists of four main stages schematically illustrated in Figure 10: (i) The synthesis of 5′-biotinylated-poly(dG)-poly(dC) molecules. The synthesis includes a 5′biotin–$(dG)_{12}$-$(dC)_{12}$ template-primer extension in the presence of dGTP and dCTP by Klenow exo$^-$ (39) (Figure 10A); (ii) Formation of a complex between the avidin and four biotinylated poly(dG)-poly(dC) molecules (Figure 10B); (iii) Separation of the poly(dC) strands from poly(dG)-strands connected to the avidin (Figure 10C); (iv) Assembling of four G-strands connected to avidin into tetra-molecular G4-DNA structures (Figure 10D). The above procedure yields G4-DNA molecules having an average length approximately equal to that of the parent poly(dG)-poly(dC) molecules (Figures 4 and 6). This result, together with the similar distance between adjacent base pairs as in dsDNA (41,42) and adjacent tetrads in G-qadruplexes (1,2,43,44), strongly suggests a tetra-molecular mechanism of G-strands assembly into G-quadruplexes.

The complex between an avidin-tetramer and four poly(dG)-poly(dC) molecules is unstable at low ionic strength and undergoes dissociation at room temperature (Figure 3). The dissociation is reversible; an increase of the ionic strength leads to almost complete reassembly of the complex. The avidin-tetramer, as well as the complex, is very stable and is not disturbed by heat or manipulations like multiple washings and dilutions (28,31,32). However, attachment of long negatively charged molecules such as DNA to the avidin can destabilize the complex. At low ionic strength the electrostatic repulsion between the DNA molecules exceeds the forces that stabilize the avidin-tetramer (hydrophobic interactions and hydrogen bonds between the sub-units). Under these conditions, the dissociation reaction becomes energetically favorable and

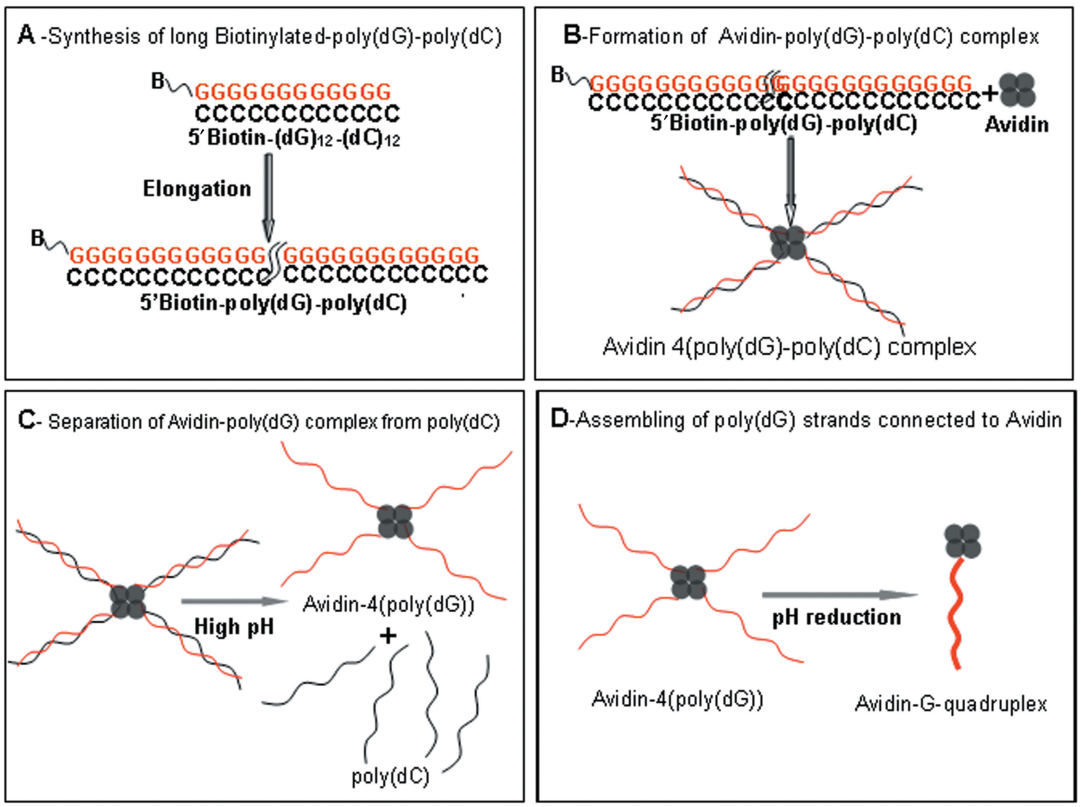

Figure 10. Scheme of tetra-molecular G4-DNA production. (**A**) The synthesis of 1.4 kbp poly(dG)-poly(dC) molecules biotin labeled at 5′-end of the poly(dG)-strand. (**B**) Formation of the complex between avidin and four biotinylated poly(dG)-poly(dC) molecules. (**C**) Separation of poly(dC) strands from biotin–poly(dG)-strands connected to avidin in 0.1 M LiOH. (**D**) Assembly of four G-strands connected to avidin into tetra-molecular G4-DNA structures.

the complex disintegrates. The increase of the ionic strength results in a reduction of the electrostatic repulsion shifting the equilibrium towards re-association of the tetramer.

We have shown that, in contrast to short G-qaudruplexes reported earlier (4,13), long mono-molecular G-quadruplexes can be formed in the absence of K^+ and Na^+ cations (18). This is true also for the long tetra-molecular G4 structures reported here. The structures made in the absence of these 'stabilizing' ions, but in the presence of nonstabilizing Li^+ are stable and do not undergo any observable change in aqueous solution for weeks. Addition of the ions to the molecules alters the CD spectrum of the DNA (Figure 8). The effect of K^+ and Na^+ on the CD properties of G4-DNA reflects changes in the fine structure of the molecules induced, by the cations.

The molecular morphology and the CD spectrum of tetra-molecular G-quadruplexes measured here are different from those reported earlier for mono-molecular G4-wires (18). The height of the former structures is notably larger than that of mono-molecular G-quadruplexes (insets of Figure 6A and B). The CD spectra of both types of molecules are also very different (Figure 8). These results are consistent with the different properties of short mono- and tetra-molecular telomeric G-quadruplexes reported in the literature (13,14). A conclusive explanation of the greater height of tetra-molecular G-quadruplexes compared to mono-molecular ones can only be given by X-ray or NMR data, which are not available for these molecules due to their complexity and only recent availability. It may originate from a stronger structural stability when all the four strands run in 3′–5′ direction rather than when every two strands run in opposite directions. Another possible explanation is that a fragment in the tetra-molecular structure located close to the site of avidin attachment is encapsulating the protein. This greater height indicates a higher resistance of the tetra-molecular structures to deformations caused by an interaction of the molecules with the mica surface and with the AFM cantilever than that of the mono-molecular G4-DNA. We have shown by EFM, (Figure 9) that tetra-molecular G-quadruplexes are characterized by a clear polarizability which is indicative of possible electrical conductivity. The high resistance of the tetra-molecular G-quadruplexes to mechanical deformations together with their electrical polarizability makes these structures very promising for nanoelectronic applications.

ACKNOWLEDGEMENTS

This work was supported by the EC through contracts IST-2001-38951 ('DNA-Based Nanowires') and FP6-029192 ('DNA-Based Nanodevices'). Funding to pay the Open Access publication charges for this article was provided by a European Grant FP6-029192 ('DNA-Based Nanodevices').

Conflict of interest statement. None declared.

REFERENCES

1. Laughlan,G., Murchie,A.I.H., Norman,D.G., Moore,M.H., Moody,P.C.E., Lilley,D.M.J. and Luisi,B. (1994) The high-resolution crystal structure of a parallel-stranded guanine tetraplex. *Science*, **265**, 520–524.
2. Phillips,K., Dauter,Z., Murchie,A.I.H., Lilley,D.M.J. and Luisi,B. (1997) The crystal structure of a parallel-stranded guanine tetraplex at 0.95 angstrom resolution. *J. Mol. Biol.*, **273**, 171–182.
3. Parkinson,G.N., Lee,M.P. and Neidle,S. (2002) Crystal structure of parallel quadruplexes from human telomeric DNA. *Nature (Lond.)*, **417**, 876–880.
4. Burge,S., Parkinson,G.N., Hazel,P., Todd,A.K. and Neidle,S. (2006) Quadruplex DNA: sequence, topology and structure. *Nucleic Acids Res.*, **34**, 5402–5415.
5. Gu,J. and Leszczynski,J. (2002) Origin of Na+/K+ selectivity of the guanine tetraplexes in water: the theoretical rationale. *J. Phys. Chem. A.*, **106**, 529–532.
6. Sen,D. and Gilbert,W. (1992) Novel DNA superstructures formed by telomere-like oligomers. *Biochemistry*, **31**, 65–70.
7. Marsh,T.C., Vesenka,J. and Henderson,E. (1995) A new DNA nanostructure the G-wire imaged by scanning probe microscopy. *Nucleic Acids Res.*, **23**, 696–700.
8. Protozanova,E. and Macgregor,R.B. (1996) Frayed wires a thermally stable form of DNA with two distinct structural domains. *Biochemistry*, **35**, 16638–16645.
9. Kerwin,S.M. (2000) G-Quadruplex DNA as a target for drug design. *Curr. Pharmaceutic. Design*, **6**, 441–478.
10. Marathias,V.M. and Bolton,P.H. (1999) Determinants of DNA quadruplex structural type: sequence and potassium binding. *Biochemistry*, **38**, 4355–4364.
11. Sen,D. and Gilbert,W. (1992) Guanine quartet structures. *Methods Enzymol.*, **211**, 191–199.
12. Wang,Y. and Patel,D.J. (1994) Solution structure of the Tetrahymena telomeric repeat d(T2G4)4 G-tetraplex. *Structure*, **2**, 1141–1156.
13. Davis,J.T. (2004) G-quartets 40 years later: from 50-GMP to molecular biology and supramolecular chemistry. *Angew. Chem. Int.*, **43**, 668–698.
14. Simonsson,T. (2001) G-quadruplex DNA structures-variation on a theme. *Biol. Chem.*, **382**, 621–628.
15. Gros,J., Rosu,F., Amrane,S., De Cian,A., Gabelica,V., Lacroix,L. and Mergny,J.-L. (2007) Guanines are a quartet's best friend: impact of base substitutions on the kinetics and stability of tetramolecular quadruplexes. *Nucleic Acids Res.*, **35**, 3064–3075.
16. Eddy,J. and Maizels,N. (2006) Gene function correlates with potential for G4 DNA formation in the human genome. *Nucleic Acids Res.*, **34**, 3887–3896.
17. Kan,Z.-Y., Lin,Y., Wang,F., Zhuang,X.-V., Zhao,Y., Pang,D.-W., Hao,Y.-H. and Tan,Z. (2007) G-quadruplex formation in human telomeric (TTAGGG)4 sequence with complementary strand in close vicinity under molecularly crowded condition. *Nucleic Acids Res.*, **35**, 3646–3653.
18. Kotlyar,A.B., Borovok,N., Molotsky,T., Cohen,H., Shapir,E. and Porath,D. (2005) Long, monomolecular guanine-based nanowires. *Adv. Mater.*, **17**, 1901–1905.
19. Yang,X., Wang,X.-B., Vorpagel,E.R. and Wang,L.-S. (2004) Direct experimental observation of the low ionization potentials of guanine in free oligonucleotides by using photoelectron spectroscopy. *Proc. Natl Acad. Sci. USA*, **101**, 17588–17592.
20. Di Felice,R., Calzolari,A. and Zhang,H. (2004) Toward metalated DNA-based structures. *Nanotechnology*, **15**, 1256–1263.
21. Calzolari,A., Di Felice,R. and Molinari,E. (2002) G-quartet biomolecular nanowires. *Appl. Phys. Lett.*, **80**, 3331–3333.
22. Marsh,T.C. and Henderson,E. (1994) G-wires: self-assembly of a telomeric oligonucleotide, d(GGGGTTGGGG), into large superstructures. *Biochemistry*, **33**, 10718–10724.
23. Cohen,H., Sapir,T., Borovok,N., Molotsky,T., Di Felice,R., Kotlyar,A.B. and Porath,D. (2007) Polarizability of G4-DNA observed by electrostatic force microscopy measurements. *Nano Letters*, **7**, 981–986.
24. Green,N.M. (1975) Avidin. *Adv. Protein Chem.*, **29**, 85–133.
25. Wilchek,M. and Bayer,E.A. (1990) Introduction to avidin-biotin technology. *Method Enzymol.*, **184**, 5–13.

26. Livnah,O., Bayer,E.A., Wilchek,M. and Sussman,J.L. (1993) Three-dimensional structures of avidin and the avidin–biotin complex. *Proc Natl Acad. Sci. USA*, **90**, 5076–5080.
27. Wilchek,M., Bayer,E.A. and Livnah,O. (2006) Essentials of biorecognition: The (strept)avidin–biotin system as a model for protein–protein and protein–ligand interaction. *Immunol. Lett.*, **103**, 27–32.
28. Diamandis,E.P. and Christopoulos,T.K. (1991) The biotin-(strept)avidin system: principles and applications in biotechnology. *Clin. Chem.*, **37**, 625–636.
29. Wilchek,M. (2004) My life with affinity. *Protein Sci.*, **13**, 3066–3070.
30. Wilchek,M. and Bayer,E.A. (1999) Foreword and introduction to the book (strept)avidin–biotin system. *Biomol. Eng.*, **16**, 1–4.
31. González,M., Argaraña,C.E. and Fidelio,G.D. (1999) Extremely high thermal stability of streptavidin and avidin upon biotin binding. *Biomol. Eng.*, **16**, 67–72.
32. Laitinen,O.H., Marttila,A.T., Airenne,K.J., Kulik,T., Livnah,O., Bayer,E.A., Wilchek,M. and Kulomaa,M.S. (2001) Biotin induces tetramerization of a recombinant monomeric avidin. *J. Biol. Chem.*, **276**, 8219–8224.
33. Wilchek,M., Rothenberg,J.M., Reisfeld,A. and Bayer,E.A. (1990) Direct incorporation of biotin into DNA. *Method Enzymol.*, **184**, 608–812.
34. Langer,P.R., Waldrop,A.A. and Ward,D.C. (1981) Enzymatic synthesis of biotin-labeled polynucleotides: novel nucleic acid affinity probes. *Proc. Natl Acad. Sci. USA*, **78**, 6633–6637.
35. Cantor,C.R., Warshaw,M.M. and Shapiro,H. (1970) Oligonucleotide interactions. III. Circular dichroism studies of the conformation of deoxyoligonucleotides. *Biopolymers*, **9**, 1059–1077.
36. Inove,H., Sato,K. and Anzai,J. (2005) Disintegration of layer-by-layer assemblies composed of 2-iminobiotin-labled poly(ethyleneimine) and avidin. *Biomacromolecules*, **6**, 27–29.
37. Horcas,I., Fernandez,R., Gomez-Rodriguez,J.M., Colchero,J., Gomez-Herrero,J. and Baro,A.M. (2007) WSXM: A software for scanning probe microscopy and a tool for nanotechnology. *Review of Scientific Instruments*, 78, 013705.
38. Medalsy,I., Dgany,O., Sowwan,M., Cohen,H., Yukashevska,A., Wolf,S.G., Wolf,A., Koster,A., Almog,O. *et al.* (2008) SP1 protein-based nanostructures and arrays. *Nano Letters*, **8**, 473–477.
39. Kotlyar,A.B., Borovok,N., Molotsky,T., Fadeev,L. and Gozin,M. (2005) In vitro synthesis of uniform poly(dG)–poly(dC) by Klenow exo$^-$ fragment of polymerase I. *Nucleic Acids Res.*, **33**, 525–535.
40. Borovok,N., Molotsky,T., Ghabboun,J., Cohen,H., Porath,D. and Kotlyar,A. (2007) Poly(dG)-poly(dC) DNA appears shorter than Poly(dA)-poly(dT) and possibly adopts an A-related conformation on a mica surface in ambient. *FEBS Lett.*, **581**, 5843–5846.
41. Saenger,W. (1984) *Principles of Nucleic Acids Structure*. Springer, New York.
42. Franklin,R.E. and Gosling,R.G. (1953) The structure of sodium thymonucleate fibers. I. The influence of water content. *Acta Crystallog.*, **6**, 673–677.
43. Kang,C., Zhang,X., Ratliff,R., Moyzis,R. and Rich,A. (1992) Crystal structure of four-stranded Oxytricha telomeric DNA. *Nature*, **356**, 126–131.
44. Smith,F.W., Schultze,P. and Feigon,J. (1995) Solution structures of unimolecular quadruplexes formed by oligonucleotides containing Oxytricha telomere repeats. *Structure*, **3**, 997–1008.